Available online at www.sciencedirect.com

ScienceDirect

www.elsevier.com/locate/jes

JES JOURNAL OF ENVIRONMENTAL SCIENCES

www.jesc.ac.cn

Sorption mechanism of naphthalene by diesel soot: Insight from displacement with phenanthrene/*p*-nitrophenol

Wenhao Wu[1,2,3,**], *Yun Huang*[1,2,3,**], *Daohui Lin*[1,2,3], *Kun Yang*[1,2,3,*]

[1] *Department of Environmental Science, Zhejiang University, Hangzhou 310058, China*
[2] *Key Laboratory of Environmental Pollution and Ecological Health of Ministry of Education, Hangzhou 310058, China*
[3] *Zhejiang Provincial Key Laboratory of Organic Pollution Process and Control, Hangzhou 310058, China*

ARTICLE INFO

Article history:
Received 20 August 2020
Revised 15 January 2021
Accepted 15 January 2021
Available online 1 February 2021

Keywords:
Competitive sorption
Diesel soot
Organic compounds
Linearity
External surface

ABSTRACT

The nonlinear sorption of hydrophobic organic contaminants (HOCs) could be changed to linear sorption by the suppression of coexisting solutes in natural system, resulting in the enhancement of mobility, bioavailability and risks of HOCs in the environment. In previous study, inspired from the competitive adsorption on activated carbon (AC), the displaceable fraction of HOCs sorption to soot by competitor was attributed to the adsorption on elemental carbon fraction of soot (EC-Soot), while the linear and nondisplaceable fraction was attributed to the partition in authigenic organic matter of soot (OM-Soot). In this study, however, we observed that the linear and nondisplaceable fraction of HOC (naphthalene) to a diesel soot (D-Soot) by competitor (phenanthrene or *p*-nitrophenol) should be attributed to not only the linear partition in OM-Soot, but also the residual linear adsorption on EC-Soot. We also observed that the competition on the surface of soot dominated by external surface was different from that of AC dominated by micropore surface, i.e., complete displacement of HOCs by *p*-nitrophenol could occur for the micropore surface of AC, but not for the external surface of soot. These observations were obtained through the separation of EC-Soot and OM-Soot from D-Soot with organic-solvent extraction and the sorption comparisons of D-Soot with an AC (ACF300) and a multiwalled carbon nanotube (MWCNT30). The obtained results would give new insights to the sorption mechanisms of HOCs by soot and help to assess their environmental risks.

Introduction

As the increasing productions and applications of organic chemicals, more and more hydrophobic organic contaminants (HOCs) such as polycyclic aromatic hydrocarbons (PAHs) are released into the natural environment, which are toxic, carcinogenic, mutagenic and have highly environmental risks (Kong et al., 2021). Sorption of HOCs by geo-sorbents could be regarded as an essential process that determine the

* Corresponding author
E-mail: kyang@zju.edu.cn (K. Yang).
** These authors contributed equally to this work.

https://doi.org/10.1016/j.jes.2021.01.017
1001-0742/

transport, bioavailability and risks of HOCs in natural systems (Cornelissen et al., 2005). Soot, as the gas condensates produced from incomplete combustion of biomass/fossil fuels and with an annual output of 17 million tons, is ubiquitous in natural environments (Hammes et al., 2007; Kuang et al., 2020; Li et al., 2018; Pignatello et al., 2017; Sigmund et al., 2018). This carbonaceous geo-sorbent has received increasing attention because of the highly nonlinear sorption for many hydrophobic organic contaminants (HOCs), 1–3 orders of magnitude higher than that to natural organic matters especially at relatively low HOC concentrations (Cornelissen et al., 2005). The highly nonlinear sorption was attributed to the unique surface porosities of spherical graphitic component of soot for adsorption, analogous to the adsorption on activated carbon (Endo et al., 2009; Jonker and Koelmans, 2002; Su et al., 2018). Therefore, soot as one of the carbonaceous geo-sorbents, was suggested to be at least one of the causes of the nonlinear sorption and may significantly affect the sequestration and bioavailability of HOCs in natural environments especially at low HOC concentrations (Endo et al., 2009; Jonker and Koelmans, 2002; Lu et al., 2016; Nguyen and Ball, 2006; Su et al., 2018; Xia et al., 2016; Zhi and Liu, 2018). Quantifying the nonlinear sorption and exploring the underlying mechanism of HOCs by soot are critical to addressing its potential impact on the fates and environmental risks of HOCs in natural systems (Chiou et al., 2015; Cornelissen et al., 2005; Pignatello et al., 2017; Xia et al., 2016).

In addition to the unique surface porosities of spherical graphitic component (i.e., elemental carbon fraction) of soot for adsorption, soot contains commonly authigenic organic matter (e.g., saturated and unsaturated hydrocarbons), which could serve as partition phase (Chen and Huang, 2011; Chiou et al., 2015; Endo et al., 2009; Hong et al., 2003; Li et al., 2018; Nguyen and Ball, 2006; Zhi and Liu, 2018). Sorption of HOCs by soot is widely regarded to be the combination of nonlinear adsorption on the elemental carbon fraction of soot and linear partition in the authigenic organic matter of soot (Chiou et al., 2015; Endo et al., 2009; Nguyen and Ball, 2006). However, the isotherm nonlinearity of HOCs sorption by soot could be reduced in the real environment, where other HOCs commonly co-exist and act as sorptive competitors. For example, Bucheli and Gustafsson (2000) observed that the isotherm linearity of pyrene sorption by soot in mixed-solute system increased as compared with that in single-solute system, indicated by the increased Freundlich linearity parameter. Sorption isotherms of *o*-xylene/1,2,3-trichlorobenzene by soot were changed from nonlinear to linear with the addition of saturated *p*-nitrophenol as competitor (Chiou et al., 2015). In natural environment, multiple HOCs commonly coexisted at relatively low concentrations. The nonlinear sorption of HOCs will be changed to linear sorption by the suppression of coexisting solutes, resulting in the enhancement of mobility and bioavailability of HOCs and the higher risks in the environment (Chiou and Kile, 1998). As known, the partition of HOCs in authigenic organic matter of soot is linear and noncompetitive, while the adsorption of HOCs on elemental carbon fraction of soot is nonlinear and competitive (Chiou and Kile, 1998; Chiou et al., 1979; Li et al., 2013; Xing et al., 1996). Thus, the isotherm nonlinearity change of HOCs with competitors by soot should be attributed to the competitive suppression of nonlinear adsorption fraction. In previous study (Chiou et al., 2015), the almost complete displacement of *o*-xylene/1,2,3-trichlorobenzene by saturated *p*-nitrophenol on an activated carbon (AC) was used to support the complete displacement of nonlinear adsorption on the elemental carbon fraction of soot. It was concluded that the linear and nondisplaceable sorption of *o*-xylene/1,2,3-trichlorobenzene with saturated *p*-nitrophenol by soot was attributed to the partition in the authigenic organic matter of soot (Chiou et al., 2015). However, the surface structure of soot dominated by external surface (i.e., the surface of mesopore/macropore and other external surface) is different from that of AC dominated by micropore surface (Galarneau et al., 2018; Gauden et al., 2006; Nguyen and Ball, 2006; NIST, 2013a, 2013b; Yang et al., 2018). Whether the complete displacement of nonlinear adsorption obtained from AC is applicable for soot or not needs to be further investigated. It was noticed that competitive adsorption of HOCs with competitor depended on the surface structures of adsorbents. For example, complete adsorption displacements of *o*-xylene/1,2,3-trichlorobenzene by saturated *p*-nitrophenol were observed on micropore surface-dominated AC (Chiou et al., 2015), but incomplete adsorption displacement of naphthalene by saturated 2,4-dichlorophenol or 4-chloroaniline on external surface-dominated carbon nanotubes (CNTs) (Yang et al., 2010). Moreover, the nonlinear adsorption isotherms of naphthalene with saturated competitors by CNTs also became linear due to the multilayer adsorption of naphthalene and competitors (Yang et al., 2006, 2010). Thus, instead of the complete adsorption displacement of HOCs by competitor on micropore surface-dominated AC (Chiou et al., 2015), incomplete adsorption displacement and linear isotherm of residual HOCs adsorption could be observed on the elemental carbon fraction of external surface-dominated soot (Nguyen and Ball, 2006; NIST, 2013a, 2013b). Therefore, we hypothesize that the linear and nondisplaceable sorption of HOCs with saturated competitors by soot could be attributed to not only the linear partition in authigenic organic matter of soot, but also the residual linear adsorption on elemental carbon fraction of soot. To the best of our knowledge, the important role of the residual linear adsorption in the linear sorption of HOCs by soot under competition has not been reported in previous studies.

To verify the hypothesis proposed above, elemental carbon fraction (adsorption phase, EC-Soot) of a diesel soot (D-Soot) was obtained by removing authigenic organic matter (partition phase, OM-Soot) through organic-solvent extraction. Adsorption of a model organic compound (naphthalene) with a nonpolar (phenanthrene) or a polar (*p*-nitrophenol) saturated organic competitor on EC-Soot was conducted to exam the contribution of residual linear adsorption to the linear isotherm of naphthalene by soot under competition. Sorption of naphthalene with competitors by OM-Soot and D-Soot were used to respectively represent the linear partition fraction and the overall linear sorption under competition. AC and CNT are adsorbents mainly with micropore surface and external surface, respectively. Adsorption of naphthalene and displacement with saturated competitors on AC and CNT were also conducted to investigate the displacements on micropore/external surface and their influences on the residual linear adsorption, and to compare with soot.

Table 1 – Selected physicochemical properties of compounds.

Compound	MW (g/mol)	MP (°C)	logK_{ow}	S_w (mg/L)	V_I/100 (mg/mol)	π^*	β_m	α_m	λ_{max} (nm)	pK_a
Naphthalene	123.18	80.2	3.3	31.7	0.753	0.70	0.15	0	E_x:218 E_m:324	/
Phenanthrene	178.23	101	4.57	1.29	1.015	0.80	0.20	0	E_x:250 E_m:366	/
p-Nitrophenol	139.11	113	1.79	16,000	0.685	1.01	0.32	0.93	317	7.15

MW: molecular weight; MP: melting points; logK_{ow}: octanol/water distribution coefficient; S_w: water solubility; V_I/100: intrinsic molar volume; π^*: polarity/polarizability parameter; β_m: hydrogen-bonding acceptor parameter; α_m: hydrogen-bonding donor parameter; λ_{max}: maximum absorption wavelength; pK_a: dissociated constant; E_x: excitation wavelength; E_m: emission wavelength. All data obtained from Yang et al. (2016).

1. Materials and methods

1.1. Chemicals

Naphthalene (+99%), *p*-nitrophenol (+99.5%) and phenanthrene (+97%) were purchased from Acros Organics Co., Sinopharm Chemical Reagent Co. and Fluka Chemistry Co., respectively. The selected physicochemical properties of these chemicals are listed in Table 1. High performance liquid chromatography-grade methanol and analytical-grade dichloromethane were purchased from Thermo Fisher Scientific Co. and Sinopharm Chemical Reagent Co., respectively.

1.2. Sorbents

Diesel soot (D-Soot) was collected from the exhaust pipes of diesel engine in ships (Zhejiang, China). It was ground through 80-mesh sieve and dried at 60°C for 24 hr before use. The authigenic organic matter was extracted from D-Soot by Soxhlet extraction with dichloromethane for 18 hr till the colorless of the extractant (NIST, 2013a, 2013b). The soot after extraction (EC-Soot) was dried at 60°C for 24 hr, and grounded through 80-mesh sieve. The extractable organic matter (OM-Soot) was obtained by nitrogen blowing evaporation of the dichloromethane extractant. The weight percentages of EC-Soot and OM-Soot in D-Soot are 92.2% and 7.8%, respectively. Activated carbon (Filtrasorb 300, ACF300) was obtained from Calgon Carbon Co. Multiwalled carbon nanotube (MWCNT30) with purity of +98% and outer diameter of 20–30 nm was supplied by Chengdu Organic Chemistry Co.

1.3. Sorbent characterization

The C, H, and N contents of D-Soot, EC-Soot, OM-Soot, ACF300 and MWCNT30 were measured by an elemental analyzer (FlashEA1112, Thermo Finningan, USA). The ash contents of sorbents were determined by the residue mass after 800°C in thermal gravimetric analysis (TG, **Fig. S1**). TG analysis was conducted by a thermal analysis instrument (SDTQ600, TA Instruments, USA) with a heating rate of 10°C/min and a flow rate of 120 mL/min in air atmosphere. The O content was calculated by mass difference. The surface area and pore size distribution of D-Soot, EC-Soot, ACF300 and MWCNT30 were calculated from N_2 sorption-desorption isotherms at 77 K using a physisorption analyzer (AUTOSORB-1, Quantachrome, USA) (**Fig. S2**). The surface area (SA) and the external surface area (S_{ext}) were estimated by the multipoint Brunaer-Emmett-Teller (BET) method and the *V-t* method, respectively. The micropore volume (V_{micro}) and total pore volume (V_{total}) were calculated by the density functional theory (DFT) method. The selected physicochemical properties of these sorbents are listed in Table 2. The morphologies of diesel soot before and after organic-solvent extraction (i.e., D-Soot and EC-Soot) were characterized using scanning electron microscope (SEM, SU8010, Hitachi, Japan) and transmission electron microscope (TEM, JEM-1230, JEOL, Japan) techniques. The SEM and TEM images show that D-Soot and EC-Soot are both comprised of spherical particles (Fig. 1). The diameters of D-Soot and EC-Soot particles showed in the TEM images are 44 ± 8 and 36 ± 7 nm, respectively. The slight decrease of particle diameter of diesel soot after organic-solvent extraction could be attributed to the removal of authigenic organic matter (Hong et al., 2003; Nguyen and Ball, 2006). The details and diagrams of characterization processes are provided in Appendix A. Supplementary data.

1.4. Sorption experiments

Sorption experiments in single or binary systems were conducted using a batch equilibration technique at 25 ± 1°C. In single-solute system, a certain amount (5–25 mg) of sorbent with background solution containing 0.01 mol/L $CaCl_2$ were added into 8 or 40 mL screw vials. Naphthalene was first dissolved in methanol and injected into background solution with volume ratio of methanol below 0.1% to avoid the co-solvent effect. Solid-to-solution ratios were adjusted to ensure the removal rates of naphthalene over 20%. The mixtures in vials were shaken at 150 r/min for 7 days to reach equilibrium. In bi-solute system, the procedures of sorption experiment were the same with that of single-solute sorption experiment, except for the addition of competitor (i.e., phenanthrene or *p*-nitrophenol) into background solution. The equilibrium concentration of competitor was controlled to its water solubility (Table 1) by adding excess amount of competitor to achieve the maximum competition (Chiou et al., 2015; Wang et al., 2006; Yang et al., 2006). The equilibrium pH values of both single-solute and bi-solute systems were adjusted to 5.0 using 0.1 mol/L HCl or 0.1 mol/L NaOH solution. After equilibration, the vials were centrifuged at 3500 r/min for 20 min. Solutes in the supernatant were analyzed by a reverse-phase

Table 2 – Selected physicochemical properties of D-Soot, EC-Soot, OM-Soot, ACF300 and MWCNT30.

Sample	SA (m^2/g)	S_{ext} (m^2/g)	V_{micro} (cm^3/g)	V_{tot} (cm^3/g)	R_{micro} (%)	C (wt.%)	H (wt.%)	N (wt.%)	O (wt.%)	H/C	O/C	Ash (wt.%)
D-Soot	31.5	31.5	0.00409	0.044	9.3	61.2	2.03	0.61	21.9	0.40	0.27	14.2
EC-Soot	60.4	59.8	0.00458	0.192	2.4	60.3	1.54	0.55	22.5	0.31	0.28	15.0
OM-Soot	ND	ND	ND	ND	ND	70.3	8.22	0.90	15.9	1.40	0.17	4.71
ACF300	813	185	0.305	0.414	74	84.4	1.07	0.24	6.37	0.15	0.06	7.91
MWCNT30	163	163	0.00660	0.603	1.1	95.9	0.52	0.13	3.43	0.07	0.03	0.03

D-Soot: diesel soot; EC-Soot: elemental carbon fraction of diesel soot; OM-Soot: authigenic organic matter of diesel soot; ACF300: activated carbon (Filtrasorb 300); MWCNT30: multiwalled carbon nanotube with outer diameter of 20–30 nm; SA: surface area estimated by Brunaer-Emmett-Teller (BET) method; S_{ext}: external surface area calculated by *V-t* method; V_{micro}: micropore volume calculated by the density functional theory (DFT) method; V_{tot}: total pore volume calculated by the DFT method; R_{micro}: the ratio of micropore pore volume to total pore volume; H/C: atomic ratio of hydrogen to carbon; O/C: atomic ratio of oxygen to carbon; ND: not detected. The ash content of was determined by residue mass after 800°C in the thermal gravimetric analysis.

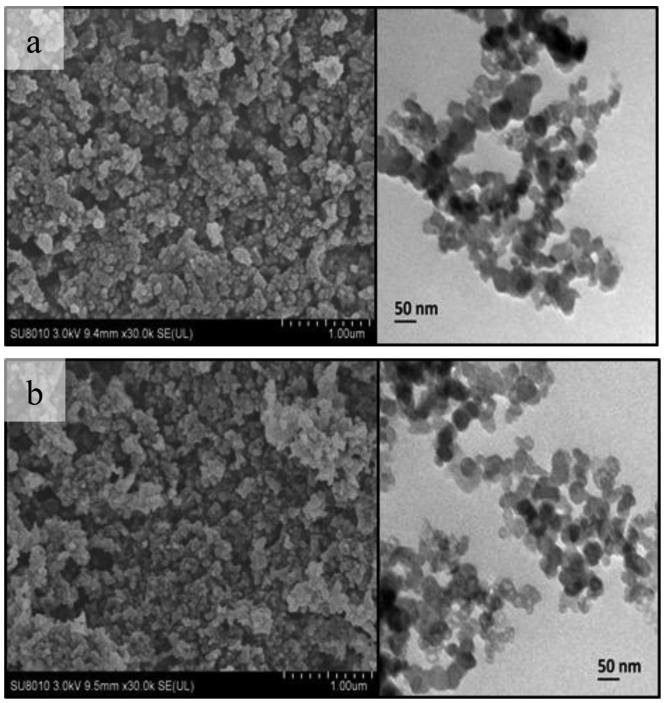

Fig. 1 – Scanning electron microscope (SEM, Left) images and transmission electron microscope (TEM, Right) images of (a) D-Soot and (b) EC-Soot.

liquid chromatography (LC 20A series, Shimadzu, Japan, XDB-C18, 4.6 mm × 150 mm) equipped with both UV detector (for *p*-nitrophenol, Table 1) and fluorescence detector (for naphthalene and phenanthrene, Table 1). The mobile phase was the 90:10 (*V*/*V*) mixture of methanol and water at a flow rate of 1 mL/min. Experimental uncertainties evaluated in vials were less than 4% of the initial chemical concentrations. Therefore, the sorbed amounts of solutes by sorbents were calculated using the mass difference in solution.

1.5. *Sorption model and isotherm fitting*

Dubinnin-Ashitakhov (DA) model (Eq. (1)) has been successfully used to fit single-solute and bi-solute sorption isotherms of organic compounds by carbonaceous sorbents in previous studies (Dubinin and Astakhov, 1971; Wu et al., 2016; Yang and Xing, 2010), and thus was employed to fit the sorption data in this study. The linear isotherms of naphthalene under competition were also fitted by linear model (Eq. (2)).

$$\log\ q_e = \log\ Q^0 - (\varepsilon/E)^b \quad (1)$$

$$q_e = K_d \times C_e \quad (2)$$

where q_e (mg/g) is the sorbed amount of solute at equilibrium; Q^0 (mg/g) is the sorption capacity of solute; ε (kJ/mol) is the effective sorption potential calculated by $\varepsilon = RT\ln(C_s/C_e)$; C_e (mg/L) is the equilibrium concentration of solute; C_s (mg/L) is the water solubility of solute; R (8.314×10^{-3} kJ/(mol•K)) is the universal gas constant; T (K) is the absolute temperature; E (kJ/mol) and b are fitted parameters that can be used to identify the sorption affinity of solute (Wu et al., 2016; Yang and

Table 3 – DA and linear model fitted isotherms of naphthalene in the absence and presence of competitor (phenanthrene/*p*-nitrophenol) by sorbents.

Sorbents	Competitor	DA model					Linear model		
		Q^0 (mg/g)	*E* (kJ/mol)	*b*	r^2	MWSE	K_d	r^2	MWSE
D-Soot	None	14.7±1.2	7.29±0.30	0.99±0.04	0.997	0.0047	/	/	/
D-Soot	Phenanthrene	12.5±1.4	5.89±0.37	0.99±0.05	0.997	0.0067	0.400±0.001	0.998	0.0134
D-Soot	*p*-Nitrophenol	8.40±0.80	5.52±0.22	0.98±0.05	0.997	0.0030	0.278±0.005	0.996	0.0026
EC-Soot	None	10.3±0.3	8.93±0.12	1.06±0.02	0.999	0.0009	/	/	/
EC-Soot	Phenanthrene	8.79±0.30	5.78±0.09	0.95±0.03	0.999	0.0057	0.270±0.001	0.999	0.0043
EC-Soot	*p*-Nitrophenol	5.58±0.53	5.67±0.30	0.96±0.05	0.997	0.0052	0.169±0.003	0.997	0.0067
OM-Soot	None	83.0±7.8	5.49±0.26	0.99±0.04	0.999	0.0013	2.49±0.02	0.999	0.0049
OM-Soot	Phenanthrene	68.4±12.9	6.30±0.52	1.16±0.11	0.997	0.0035	2.72±0.03	0.999	0.0059
OM-Soot	*p*-Nitrophenol	63.9±13.5	5.61±0.63	1.02±0.12	0.994	0.0118	2.04±0.03	0.998	0.0214
ACF300	None	337±13	22.5±0.3	2.07±0.11	0.986	0.0094	/	/	/
ACF300	*p*-Nitrophenol	26.9±2.2	5.74±0.23	1.02±0.05	0.994	0.0100	0.867±0.008	0.997	0.0237
MWCNT30	None	37.2±0.4	14.9±0.2	1.03±0.02	0.999	0.0058	/	/	/
MWCNT30	*p*-Nitrophenol	16.3±2.2	5.18±0.35	0.99±0.06	0.993	0.0108	0.467±0.007	0.995	0.0435

All estimated parameter values and their standard errors were determined by data analysis software (Origin 8.5). Q^0: the sorption capacity of solute; *E* and *b*: fitted parameters that can be used to identify the sorption affinity of solute; r^2: correlation coefficient; MWSE: mean weighted square error; K_d: sorption coefficient of linear sorption; /: not applicable.

Xing, 2010); K_d (L/g) is the sorption coefficient of linear sorption. The linear model is a special form of DA model, where $b = 1$ and $E = 5.71$ kJ/mol (Yang and Xing, 2010). Mean weighted square error (MWSE, Eq. (3)), and correlation coefficients (r^2) were used to evaluate the goodness of isotherm fitting by sorption model.

$$\mathrm{MWSE} = \frac{\sum\left(\frac{q_{\mathrm{measured}} - q_{\mathrm{model}}}{q_{\mathrm{measured}}}\right)^2}{v} \quad (3)$$

where q_{measured} is the sorbed amount measured by experiment; q_{model} is the sorbed amount calculated by sorption model; v is the degree of freedom ($v = N$-3 for DA model; $v = N$-1 for linear model); N is the number of experimental data points. All estimated model parameter values were obtained by a commercial software (Origin 8.5).

2. Results and discussion

Isotherms of naphthalene with or without competitor (i.e., phenanthrene or *p*-nitrophenol) by D-Soot, EC-Soot and OM-Soot in Fig. 2 were fitted well with DA model, as indicated by the high correlation coefficient (r^2) and the low MWSE values (Table 3). The DA-fitted sorption capacity Q^0 of naphthalene by D-Soot was 14.7 ± 1.2 mg/g in single-solute system. The value of Q^0 decreased to 12.5 ± 1.4 and 8.40 ± 0.80 mg/g in the presence of saturated phenanthrene and *p*-nitrophenol, respectively, indicating that *p*-nitrophenol (43%) exhibits stronger competition to naphthalene than phenanthrene (15%) (Table 3). The isotherm became linear as *E* and *b* values decreased to 5.71 and 1.0, respectively (Wu et al., 2016; Yang and Xing, 2010). As the DA-fitted *b* values were close to 1.0 for all single-solute and bi-solute isotherms of naphthalene by D-Soot, EC-Soot and OM-Soot (Table 3), the isotherm linearity can be identified by the DA-fitted *E* value alone. Isotherm of naphthalene by D-Soot was changed from nonlinear to linear under competition, as the DA-fitted *E* value decreased from 7.29 ± 0.30 (> 5.71) for naphthalene in single-solute system to 5.89 ± 0.37 and 5.52 ± 0.22 (≈ 5.71) in the presence of saturated phenanthrene and *p*-nitrophenol, respectively (Table 3). Moreover, the bi-solute isotherm of naphthalene can also be well fitted by linear model (Table 3). The isotherm changed from nonlinear to linear for organic compound by soot under competition was consistent with previous studies (Bucheli and Gustafsson, 2000; Chiou et al., 2015).

Since the D-Soot is composed of EC-Soot (92.2%) and OM-Soot (7.8%), the sorption amounts of naphthalene by D-Soot ($q_{\mathrm{D\text{-}Soot/cal}}$) in single-solute/bi-solute system were calculated from the sorption amounts of naphthalene by EC-Soot ($q_{\mathrm{EC\text{-}Soot}}$) and OM-Soot ($q_{\mathrm{OM\text{-}Soot}}$) using the equation (i.e., $q_{\mathrm{D\text{-}Soot/cal}} = 92.2\% \times q_{\mathrm{EC\text{-}Soot}} + 7.8\% \times q_{\mathrm{OM\text{-}Soot}}$). Considering the experimental errors, the calculated sorption isotherms are almost overlapped with the experimental sorption isotherms of naphthalene by D-Soot in all the single-solute and bi-solute systems (Fig. 3). It was suggested that the sorption of naphthalene by D-Soot could be mainly attributed to the adsorption on elemental carbon fraction of D-Soot (i.e., EC-Soot) and the partition in authigenic organic matter of D-Soot (i.e., OM-Soot). Isotherms of naphthalene with or without saturated competitors (i.e., phenanthrene or *p*-nitrophenol) by OM-Soot are all linear and overlapped (Fig. 2c). The linear and noncompetitive isotherms of naphthalene with competitors by OM-Soot agree with the partition mechanism for HOCs (Chiou and Kile, 1998; Li et al., 2013; Schreiter et al., 2018; Xing et al., 1996). Obviously, the linear partition fraction is an important contribution to the linear isotherm of naphthalene by D-Soot under competition (Fig. 3). The DA-fitted sorption capacity Q^0 of naphthalene by EC-Soot was 10.3 ± 0.3 mg/g in single-solute system. The value of Q^0 partially decreased to 8.79 ± 0.30 and 5.58 ± 0.53 mg/g in the presence of saturated phenanthrene and *p*-nitrophenol, respectively (Table 3). Isotherm of naphthalene without competitor by EC-Soot was nonlinear as indicated by the DA-fitted *E* value of 8.93 ± 0.12 (> 5.71, Table 3). The isotherm was changed to linear un-

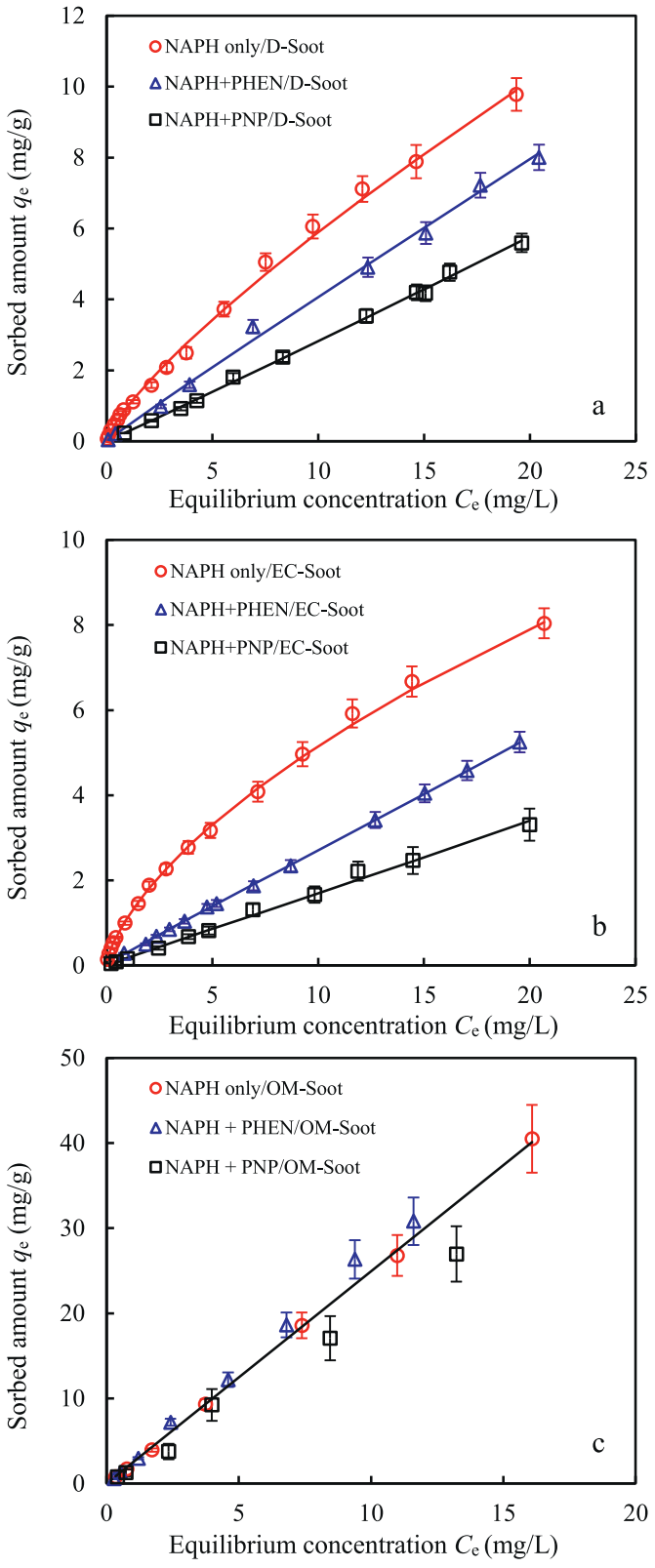

Fig. 2 – Isotherms of naphthalene (NAPH) in the absence and presence of phenanthrene (PHEN) or *p*-nitrophenol (PNP) by (a) D-Soot, (b) EC-Soot and (c) OM-Soot. Solid lines are fitted isotherms by Dubinnin-Ashitakhov (DA) model.

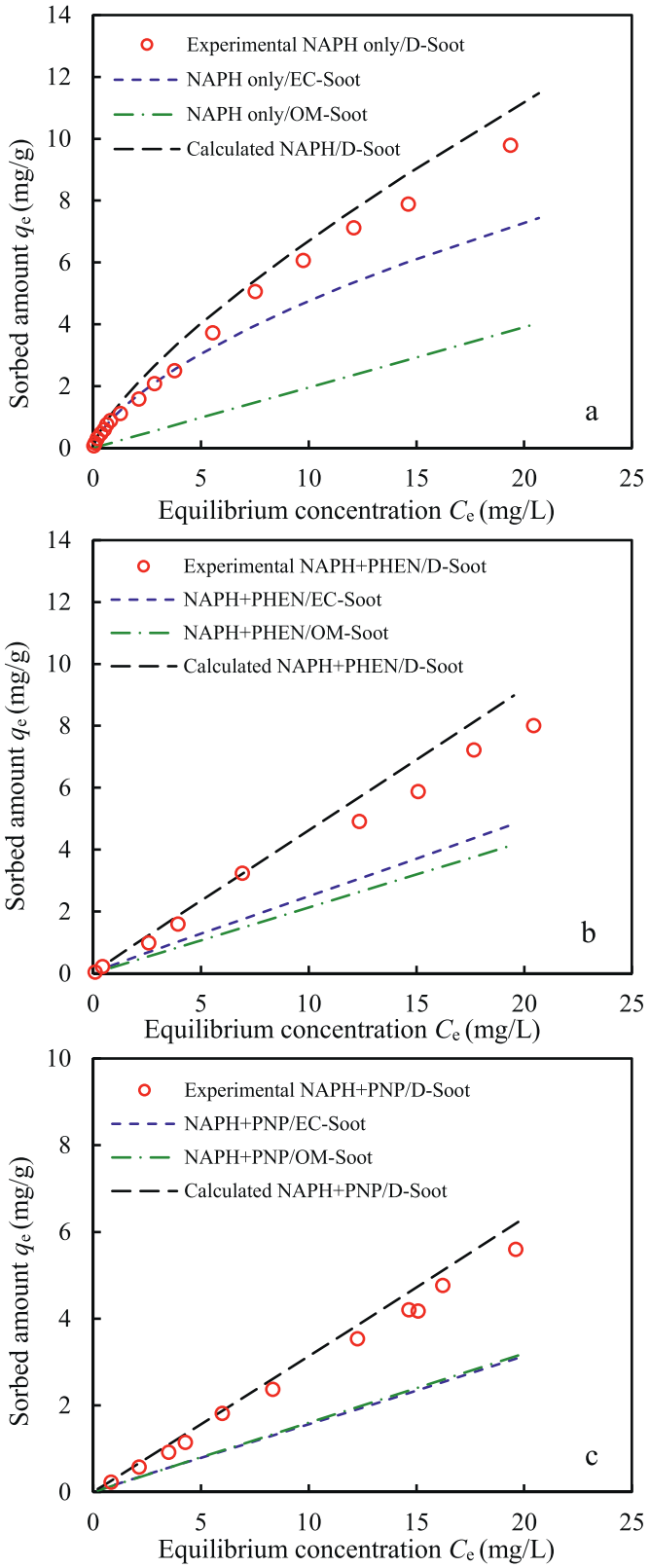

Fig. 3 – Comparison of the calculated isotherms of naphthalene (NAPH) by D-Soot using equation ($q_{D\text{-}Soot/cal}$ = 92.2% × $q_{EC\text{-}Soot}$ + 7.8% × $q_{OM\text{-}Soot}$) and the experimental isotherms. $q_{D\text{-}Soot/cal}$ is the calculated sorbed amounts by D-Soot; $q_{EC\text{-}Soot}$ and $q_{OM\text{-}Soot}$ are the experimental sorbed amounts by EC-Soot and OM-Soot, respectively. (a) NAPH only, (b) NAPH + PHEN (phenanthrene), (c) NAPH + PNP (*p*-nitrophenol).

der competition as the *E* value decreased to 5.78 ± 0.09 and 5.67 ± 0.30 (≈ 5.71) in the presence of saturated phenanthrene and *p*-nitrophenol, respectively (Table 3). Meanwhile, the bi-solute isotherms of naphthalene by EC-Soot can be well fitted by linear model (Table 3). D-Soot is composed of EC-Soot and OM-Soot. The residual linear isotherms of naphthalene with saturated competitors by D-Soot are significantly higher than the linear isotherm by OM-Soot (Fig. 3b and c). The higher sorption of naphthalene by D-Soot than that by OM-Soot should be attributed to the residual linear adsorption on EC-Soot. Therefore, the residual linear sorption of naphthalene on EC-Soot under the incomplete competition of saturated phenanthrene/*p*-nitrophenol could be another important contribution to the linear isotherm of naphthalene by D-Soot under competition, in addition to the linear partition in OM-Soot.

The nonlinear single-solute isotherm and significantly competitive sorption of naphthalene with phenanthrene/*p*-nitrophenol by D-Soot and EC-Soot are consistent with the adsorption mechanism for HOCs (Chiou and Kile, 1998; Li et al., 2013; Schreiter et al., 2018; Xing et al., 1996). Adsorption of naphthalene with or without saturated *p*-nitrophenol were also conducted on ACF300 and MWCNT30 (Fig. 4). The nonlinear adsorption of naphthalene in single-solute system on ACF300 was almost completely suppressed by saturated *p*-nitrophenol, in company with 92% decrease of adsorption capacity (Fig. 4a, Table 3). The significant decrease of HOC adsorption on AC could be attributed to the almost complete displacement of HOCs by saturated *p*-nitrophenol (Chiou et al., 2015). However, the nonlinear adsorption of naphthalene in single-solute system on MWCNT30 was incompletely displaced by saturated *p*-nitrophenol, in company with 56% decrease of adsorption capacity (Fig. 4b, Table 3). Meanwhile, the isotherm of naphthalene on MWCNT30 was changed from nonlinear to linear by competition (Fig. 4b). The residual adsorption of naphthalene on MWCNTs by incomplete displacement of competitor and the change of isotherm linearity could be interpreted by the multilayer adsorption mechanism, according to our previous study (Yang et al., 2010). The different competitive adsorption behaviors of naphthalene with saturated *p*-nitrophenol on MWCNT30 and ACF300 could be attributed to their different surface structure, where MWCNT30 is dominated by external surface while ACF300 is dominated by micropore surface (Table 3). Multilayer adsorption of HOCs with competitors could occur on the external surface of adsorbents (Yang et al., 2006, 2010), but could not occur on the micropore surface due to the limited space in micropores. It is reasonable that the micropore-dominated sorption of naphthalene on ACF300 was almost completely displaced by saturated *p*-nitrophenol, while the external surface-dominated sorption on MWCNT30 were incompletely displaced. Hence, the complete displacement of HOCs by competitors could occur on micropore surface, while the incomplete displacement could occur on external surface. Be aware that adsorption of naphthalene on ACF300 was not 100% displaced by saturated *p*-nitrophenol and the residual isotherm was also linear (Fig. 4a, Table 3). This phenomenon could be attributed to the existence of a small portion of external surface for ACF300 (Table 2).

The competitive adsorption of naphthalene with saturated *p*-nitrophenol on ACF300/MWCNT30 implied that the observed residual sorption and linear isotherms of naphthalene with saturated *p*-nitrophenol on EC-Soot could be attributed to the multilayer adsorption on the external surface of EC-Soot (Table 2). Moreover, the external surface area-normalized sorption capacity (i.e., Q^0/S_{ext}) of naphthalene with saturated *p*-nitrophenol by EC-Soot (0.0933 mg/m^2) is close to that by MWCNT30 (0.100 mg/m^2) and ACF300 (0.145 mg/m^2). This indicates that the sorption of naphthalene with saturated *p*-nitrophenol by EC-Soot should mainly be an adsorption behavior (Chun et al., 2004; James et al., 2005) and confirms that EC-Soot should mainly be the elemental carbon fraction (i.e., adsorption component) of D-Soot. However, the Q^0/S_{ext} value of naphthalene with saturated *p*-nitrophenol by D-Soot (0.267 mg/m^2) is 2–3 times of that by MWCNT30 (0.100 mg/m^2) and ACF300 (0.145 mg/m^2). This result should be attributed to the noncompetitive partition of naphthalene into the authigenic organic matter of D-Soot and the competitive adsorption by the elemental carbon fraction of D-Soot (Chun et al., 2004; James et al., 2005). Therefore, the linear isotherm of naphthalene with competitors by D-Soot should be the result of both the linear partition of naphthalene in the authigenic organic matter of D-Soot and the residual linear adsorption on external surface of D-Soot due to the incomplete displacement.

The increasing isotherm linearity of naphthalene in the presence of phenanthrene/*p*-nitrophenol on EC-Soot should result from the decreasing adsorption affinity (i.e., *E*) of naphthalene by competition (Yang et al., 2010). As multilayer adsorption of naphthalene with phenanthrene/*p*-nitrophenol occurred on the external surface of EC-Soot, naphthalene was partially adsorbed on the phenanthrene/*p*-nitrophenol-coated surface of EC-Soot. The coated phenanthrene/*p*-nitrophenol on the surface of EC-Soot have less π electron than the surface of EC-Soot (Kamlet et al., 1988; Yang et al., 2010). Thus, the π-π interaction between naphthalene and the coated phenanthrene/*p*-nitrophenol on EC-Soot surface could be much weaker than that between naphthalene and uncoated EC-Soot surface. In addition, the competition of *p*-nitrophenol was stronger than phenanthrene for naphthalene adsorption on EC-Soot, indicated by the lower adsorption capacity of naphthalene with saturated *p*-nitrophenol than that with phenanthrene (Fig. 2b, Table 3). The adsorbed nonpolar phenanthrene on EC-Soot could interact with naphthalene through π-π interactions to form multilayer adsorption (Ho and Leung, 2019; Yang et al., 2006, 2010; Yu et al., 2016). It was observed in previous study that adsorption capacity of naphthalene by external surface-dominated CNTs was not significantly suppressed by the competition of saturated phenanthrene due to the multilayer adsorption (Yang et al., 2006). Thus, it is reasonable that adsorption capacity of naphthalene by external surface-dominated EC-Soot was slightly reduced (15%) by the competition of saturated phenanthrene (Fig. 2b, Table 3). The polar *p*-nitrophenol could be adsorbed on the external surface of EC-Soot by using its polar functional group (i.e., –OH) to interact with the surface through hydrogen bonds. The hydrophobic benzene ring of *p*-nitrophenol could be exposed toward the aqueous solution to adsorb naphtha-

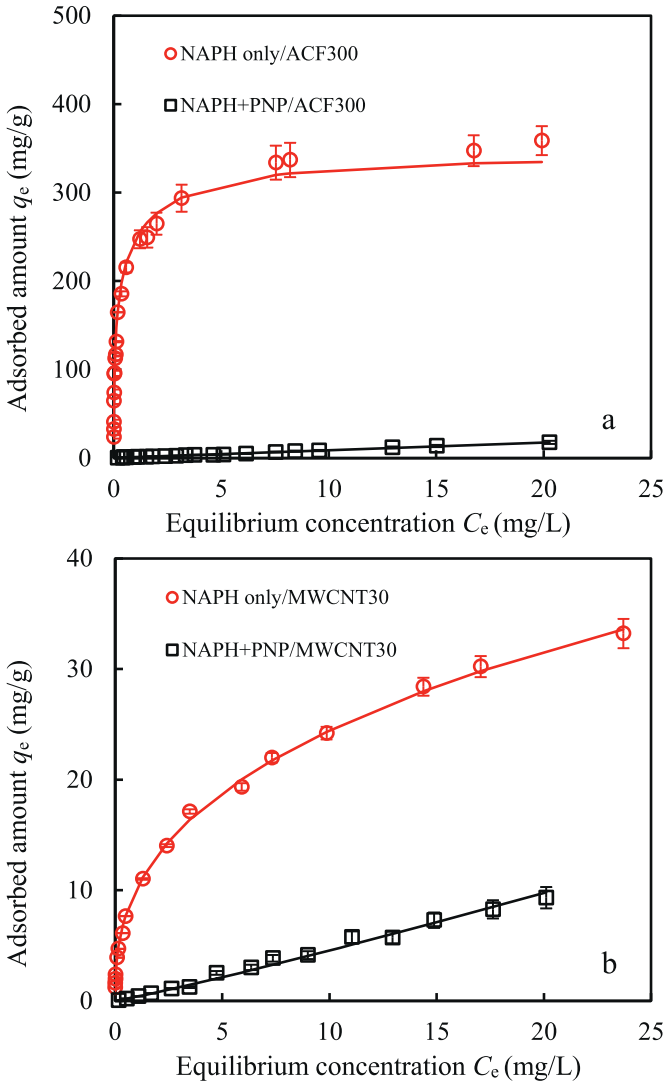

Fig. 4 – Isotherms of naphthalene (NAPH) in the absence and presence of *p*-nitrophenol (PNP) on (a) ACF300 and (b) MWCNT30. Solid lines are fitted isotherms by DA model.

lene through π-π interaction and form multilayer adsorption (Yang et al., 2006, 2010). However, part of the polar *p*-nitrophenol could also be adsorbed on the external surface of EC-Soot to interact with the surface through π-π interactions. Thus, the hydrophilic functional group (i.e., –OH) of *p*-nitrophenol could be exposed toward the aqueous solution to interact with water but not naphthalene (Chen et al., 2018; Wu et al., 2012; Yang et al., 2010). Thus, it is reasonable that adsorption capacity of naphthalene by EC-Soot was more reduced (46%) by the competition of saturated *p*-nitrophenol than phenanthrene (Fig. 2b, Table 3).

3. Conclusions

Quantifying the nonlinear sorption and understanding the sorption mechanism of HOCs by soot is of great importance to assess the transport, transformation and bioavailability of HOCs in natural environments. In this study, competitive sorption of naphthalene with saturated phenanthrene/*p*-nitrophenol by a diesel soot (D-Soot), its separated spherical graphitic component (EC-Soot) and authigenic organic matter (OM-Soot) were investigated. The incomplete displacement and isotherm linearity of naphthalene with competitors on EC-Soot indicated that the linear isotherms by soot was attributed to not only the linear partition of naphthalene in OM-Soot of soot, but also the residual linear adsorption on external surface (EC-Soot) of soot due to the incomplete displacement. Ignoring the important contribution of residual linear adsorption to the linear isotherms of HOCs by soot under competition would lead to the misunderstanding of sorption mechanism of HOCs by soot. The results obtained in this study can help to recognize the nonlinear and linear sorption behaviors of organic contaminants by soot and to access the potential risks of soot in real environment with multiple organic contaminants.

Acknowledgments

This work was supported partly by the National Natural Science Foundation of China (Nos. 21777138 and 21621005), the National Key Research and Development Program of China (No. 2017YFA0207001), and the Key Research and Development Program of Zhejiang Province (No. 2019C03105).

Appendix A. Supplementary data

Supplementary material associated with this article can be found in the online version at doi:10.1016/j.jes.2021.01.017.

REFERENCES

Bucheli, T.D., Gustafsson, Ö., 2000. Quantification of the soot-water distribution coefficient of PAHs provides mechanistic basis for enhanced sorption observations. Environ. Sci. Technol. 34, 5144–5151.

Chen, B.L., Huang, W.H., 2011. Effects of compositional heterogeneity and nanoporosity of raw and treated biomass-generated soot on adsorption and absorption of organic contaminants. Environ. Pollut. 159, 550–556.

Chen, W.F., Wei, R., Ni, J.Z., Yang, L.M., Qian, W., Yang, Y.S., 2018. Sorption of chlorinated hydrocarbons to biochars in aqueous environment: effects of the amorphous carbon structure of biochars and the molecular properties of adsorbates. Chemosphere 210, 753–761.

Chiou, C.T., Cheng, J.Z., Hung, W., Chen, B.L., Lin, T., 2015. Resolution of adsorption and partition components of organic compounds on black carbons. Environ. Sci. Technol. 49, 9116–9123.

Chiou, C.T., Kile, D.E., 1998. Deviations from sorption linearity on soils of polar and nonpolar organic compounds at low relative concentrations. Environ. Sci. Technol. 32, 338–343.

Chiou, C.T., Peters, L.J., Freed, V.H., 1979. Physical concept of soil-water equilibria for non-ionic organic-compounds. Science 206, 831–832.

Chun, Y., Sheng, G.Y., Chiou, C.T., Xing, B.S., 2004. Compositions and sorptive properties of crop residue-derived chars. Environ. Sci. Technol. 38, 4649–4655.

Cornelissen, G., Gustafsson, Ö., Bucheli, T.D., Jonker, M.T.O., Koelmans, A.A., Van Noort, P.C.M., 2005. Extensive sorption of organic compounds to black carbon, coal, and kerogen in sediments and soils: mechanisms and consequences for distribution, bioaccumulation, and biodegradation. Environ. Sci. Technol. 39, 6881–6895.

Dubinin, M.M., Astakhov, V.A., 1971. Development of the concepts of volume filling of micropores in the adsorption of gases and vapors by microporous adsorbents. Izv. Akad. Nauk SSSR Ser. Khim. 1, 5–11.

Endo, S., Grathwohl, P., Haderlein, S.B., Schmidt, T.C., 2009. Effects of native organic material and water on sorption properties of reference diesel soot. Environ. Sci. Technol. 43, 3187–3193.

Galarneau, A., Mehlhorn, D., Guenneau, F., Coasne, B., Villemot, F., Minoux, D., et al., 2018. Specific surface area determination for microporous/mesoporous materials: the case of mesoporous FAU-Y zeolites. Langmuir 34, 14134–14142.

Gauden, P.A., Szemenchtig-Gauden, E., Rychlicki, G., Duber, S., Garbacz, J.K., Buczkowski, R., 2006. Changes of the porous structure of activated carbons applied in a filter bed pilot operation. J. Colloid Interface Sci. 295, 327–347.

Hammes, K., Schmidt, M.W.I., Smernik, R.J., Currie, L.A., Ball, W.P., Nguyen, T.H., et al., 2007. Comparison of quantification methods to measure fire-derived (black/elemental) carbon in soils and sediments using reference materials from soil, water, sediment and the atmosphere. Global Biogeochem. Cycles 21, GB3016.

Ho, W., Leung, K.S., 2019. Sorption and desorption of organic UV filters onto microplastics in single and multi-solute systems. Environ. Pollut. 254, 113066–113074.

Hong, L., Ghosh, U., Mahajan, T., Zare, R.N., Luthy, R.G., 2003. PAH sorption mechanism and partitioning behavior in lampblack-impacted soils from former oil-gas plant sites. Environ. Sci. Technol. 37, 3625–3634.

James, G., Sabatini, D.A., Chiou, C.T., Rutherford, D., Scott, A.C., Karapanagioti, H.K., 2005. Evaluating phenanthrene sorption on various wood chars. Water Res. 39, 549–558.

Jonker, M.T.O., Koelmans, A.A., 2002. Sorption of polycyclic aromatic hydrocarbons and polychlorinated biphenyls to soot and soot-like materials in the aqueous environment: mechanistic considerations. Environ. Sci. Technol. 36, 3725–3734.

Kamlet, M.J., Doherty, R.M., Abraham, M.H., Marcus, Y., Taft, R.W., 1988. Linear solvation energy relationship. 46. An improved equation for correlation and prediction of octanol/water partition coefficients of organic nonelectrolytes (including strong hydrogen bond donor solutes). J. Phys. Chem. 92, 5244–5255.

Kong, J.J., Dai, Y.X., Han, M.S., He, H., Hu, J.P., Zhang, J.Y., et al., 2021. Nitrated and parent PAHs in the surface water of Lake Taihu, China: occurrence, distribution, source, and human health risk assessment. J. Environ. Sci. 102, 159–169.

Kuang, Y., Guo, Y., Chai, J.Q., Shang, J., Zhu, J.L., Stevanovic, S., et al., 2020. Comparison of light absorption and oxidative potential of biodiesel/diesel and chemicals/diesel blends soot particles. J. Environ. Sci. 87, 184–193.

Li, J.Z., Jiang, L., Xiang, X., Xu, S., Wen, R., Liu, X., 2013. Competitive sorption between 17α-ethinyl estradiol and bisphenol A/4-*n*-nonylphenol by soils. J. Environ. Sci. 25 (6), 1154–1163.

Li, M., Bao, F.X., Zhang, Y., Song, W.J., Chen, C.C., Zhao, J.C., 2018. Role of elemental in the photochemical aging of soot. Proc. Natl. Acad. Sci. U.S.A. 115, 7717–7722.

Lu, Z.J., MacFarlane, J.K., Gschwend, P.M. , 2016. Adsorption of organic compounds to diesel soot: frontal analysis and polyparameter linear free-energy relationship. Environ. Sci. Technol. 50, 285–293.

NIST, 2013a. Certificate of analysis for standard reference material 2975, diesel particulate matter (industrial forklift). Gaithersburg, MD.

NIST, 2013b. Certificate of analysis for standard reference material 1650b, diesel particulate matter (industrial forklift). Gaithersburg, MD.

Nguyen, T.H., Ball, W.P., 2006. Absorption and adsorption of hydrophobic organic contaminants to diesel and hexane Soot. Environ. Sci. Technol. 40, 2958–2964.

Pignatello, J.J., Mitch, W.A., Xu, W., 2017. Activity and reactivity of pyrogenic carbonaceous matter toward organic compounds. Environ. Sci. Technol. 51, 8893–8908.

Schreiter, I.J., Schmidt, W., Schüth, C., 2018. Sorption mechanisms of chlorinated hydrocarbons on biochar produced from different feedstocks: conclusions from single- and bi-solute experiments. Chemosphere 203, 34–43.

Sigmund, G., Jiang, C.J., Hofmann, T., Chen, W., 2018. Environmental transformation of natural and engineered carbon nanoparticles and implications for the fate of organic contaminants. Environ. Sci. Nano 5, 2500–2518.

Su, P., Kuo, D.T.F., Shih, Y., Chen, C., 2018. Sorption of organic compounds to two diesel soot black carbons in water evaluated by liquid chromatography and polyparameter linear solvation energy relationship. Water Res. 144, 709–718.

Wang, X.L., Tao, S., Xing, B.S., 2006. Competitive sorption of pyrene on wood chars. Environ. Sci. Technol. 40, 3267–3272.
Wu, W.H., Chen, W., Lin, D.H., Yang, K., 2012. Influence of surface oxidation of multiwalled carbon nanotubes on the adsorption affinity and capacity of polar and nonpolar organic compounds in aqueous phase. Environ. Sci. Technol. 46, 5446–5454.
Wu, W.H., Yang, K., Chen, W., Wang, W.D., Zhang, J., Lin, D.H., et al., 2016. Correlation and prediction of adsorption capacity and affinity of aromatic compounds on carbon nanotubes. Water Res. 88, 492–501.
Xia, H., Gomez-Eyles, J.L., Ghosh, U., 2016. Effect of polycyclic aromatic hydrocarbon source materials and soil components on partitioning and dermal uptake. Environ. Sci. Technol. 50, 3444–3452.
Xing, B.S., Pignatello, J.J., Gigliotti, B., 1996. Competitive sorption between atrazine and other organic compounds in soils and model sorbents. Environ. Sci. Technol. 30, 2432–2440.
Yang, K., Wang, X.L., Zhu, L.Z., Xing, B.S., 2006. Competitive Sorption of pyrene, phenanthrene, and naphthalene on multiwalled carbon nanotubes. Environ. Sci. Technol. 40, 5804–5810.
Yang, K., Wu, W.H., Jing, Q.F., Jiang, W., Xing, B.S., 2010. Competitive adsorption of naphthalene with 2,4-dichlorophenol and 4-chloroaniline on multiwalled carbon nanotubes. Environ. Sci. Technol. 44, 3021–3027.
Yang, K., Xing, B.S., 2010. Adsorption of organic compounds by carbon nanomaterials in aqueous phase: polanyi theory and its application. Chem. Rev. 110, 5989–6008.
Yang, K., Yang, J.J., Jiang, Y., Wu, W.H., Lin, D.H., 2016. Correlations and adsorption mechanisms of aromatic compounds on a high heat temperature treated bamboo biochar. Environ. Pollut. 210, 57–64.
Yang, X., Yi, H.H., Tang, X.L., Zhao, S.Z., Yang, Z.Y., Ma, Y.Q., et al., 2018. Behaviors and kinetics of toluene adsorption-desorption on activated carbons with varying pore structure. J. Environ. Sci. 67, 104–114.
Yu, S.J., Wang, X.X., Ai, Y.J., Tan, X.L., Hayat, T., Hu, W.P., et al., 2016. Experimental and theoretical studies on competitive adsorption of aromatic compounds on reduced graphene oxides. J. Mater. Chem. A 4, 5654–5662.
Zhi, Y., Liu, J.X., 2018. Sorption and desorption of anionic, cationic and zwitterionic polyfluoroalkyl substances by soil organic matter and pyrogenic carbonaceous materials. Chem. Eng. J. 346, 682–691.